2004

The Relationship of Field Burn Severity Measures To Satellite-derived Burned Area Reflectance Classification (Barc) Maps

Andrew T. Hudak
Rocky Mountain Research Station, ahudak@fs.fed.us

Pete Robichaud
USFS Rocky Mountain Research Station, probichaud@fs.fed.us

Terrie Jain
USFS Rocky Mountain Research Station, tjain@fs.fed.us

Penelope Morgan
University of Idaho, pmorgan@uidaho.edu

Carter Stone
University of Idaho, stonec@uidaho.edu

See next page for additional authors

Date: 2004
Source: American Society for Photogrammetry and Remote Sensing Annual Conference Proceedings. CD-ROM. p. 96-104.

THE RELATIONSHIP OF FIELD BURN SEVERITY MEASURES TO SATELLITE-DERIVED BURNED AREA REFLECTANCE CLASSIFICATION (BARC) MAPS

Andrew Hudak, Research Forester
Pete Robichaud, Research Engineer
Terrie Jain, Research Forester
USFS Rocky Mountain Research Station
Moscow, ID 83843
ahudak@fs.fed.us
probichaud@fs.fed.us
tjain@fs.fed.us
Penelope Morgan, Professor
Carter Stone, GIS Analyst
Dept. of Forest Resources
University of Idaho
Moscow, ID 83844-1133
pmorgan@uidaho.edu
stonec@uidaho.edu
Jess Clark, RS/GIS Analyst
USFS Remote Sensing Applications Center
Salt Lake City, UT 84119
jtclark@fs.fed.us

ABSTRACT

Preliminary results are presented from ongoing research on spatial variability of fire effects on soils and vegetation from the Black Mountain Two and Cooney Ridge wildfires, which burned in western Montana during the 2003 fire season. Extensive field fractional cover data were sampled to assess the efficacy of quantitative satellite image-derived indicators of burn severity. The objective of this study was to compare the field burn severity measures to the digital numbers used to produce Burned Area Reflectance Classification (BARC) maps. Canopy density was the field variable most highly correlated to BARC data derived from either SPOT Multispectral (XS) or Landsat Thematic Mapper (TM) imagery. Among the other field variables, old litter depth and duff depth correlated better with the satellite data than did old litter cover. Ash cover correlated most poorly. Old litter cover correlated better with the satellite data than did exposed mineral soil or rock cover, but combining the mineral soil and rock cover fractions into a single inorganic cover fraction improved the correlation to a comparable level. Most field variables, with the notable exception of ash, tended to vary more at low and moderate severity sites than at high severity sites. Semivariograms of the field variables revealed spatial autocorrelation across the spatial scales sampled (2 – 130 m), which the 20 m or 30 m resolution satellite imagery only weakly detected. Future analyses will be broadened to quantify burn severity characteristics in other forest types and to consider erosion processes, such as soil water infiltration following fire.

INTRODUCTION

The USDA Forest Service (USFS) and other land management agencies employ remote sensing tools to efficiently and effectively manage fire-adapted ecosystems. The USFS Remote Sensing Applications Center (RSAC) provides satellite imagery and image-derived products for managing and monitoring wildfires. Burned Area Reflectance Classification (BARC) maps produced by RSAC have proved very useful for Burned Area Emergency Rehabilitation (BAER) teams during recent fire seasons; collaboration between RSAC and BAER will expand further in the upcoming fire seasons. One widely used indicator of burn severity is the Normalized Burn Ratio (NBR), calculated as the difference between the short-wave infrared and near-infrared channels, divided by their sum. Also used is the delta NBR (dNBR), calculated by subtracting post-fire from pre-fire NBR values (Key and Benson, 2001). In a field

validation of BARC products, Bobbe et al. (2003) found the dNBR to be no more accurate than NBR. Landsat Enhanced Thematic Mapper Plus (ETM+), Landsat Thematic Mapper (TM), and SPOT Multispectral (XS) imagery are the satellite sensors most commonly used for mapping wildfires. However, failure of the scan line corrector on Landsat 7 (http://landsat7.usgs.gov/updates.php) has drastically compromised the provision of ETM+ imagery and forced greater reliance on Landat 5 TM and SPOT 4 XS imagery to map wildfires.

The two wildfires chosen for this analysis, Black Mountain Two and Cooney Ridge, were located west and east, respectively, of Missoula, Montana (Figure 1). The Black Mountain Two wildfire ignited 11 Aug 2003 and burned 2855 ha before containment on 2 Sep 2003. The Cooney Ridge wildfire ignited 8 Aug 2003 and burned 8589 ha before containment on 14 Sep 2003. Fire severities ranged from none (some areas were unburned), to low, moderate and high. The fires occurred in mixed conifer forests on complex terrain in western Montana, USA. Areas burned most severely are relatively uniform, while the heterogeneity of moderate and low severity burns is substantially higher. On the Cooney Ridge fire, severity was observed to be higher and more uniform on privately owned lands that had recently been heavily logged (Stone et al., 2004).

The objectives of this Joint Fire Science Program (JFSP) funded project are to compare alternative remote sensors and analysis approaches across a diversity of soils, vegetation, and fire conditions, and to explicitly link fire behavior, fuels and fire effects to quantitative indicators of burn severity that can be assessed in the field, predicted from fire effects models and mapped remotely.

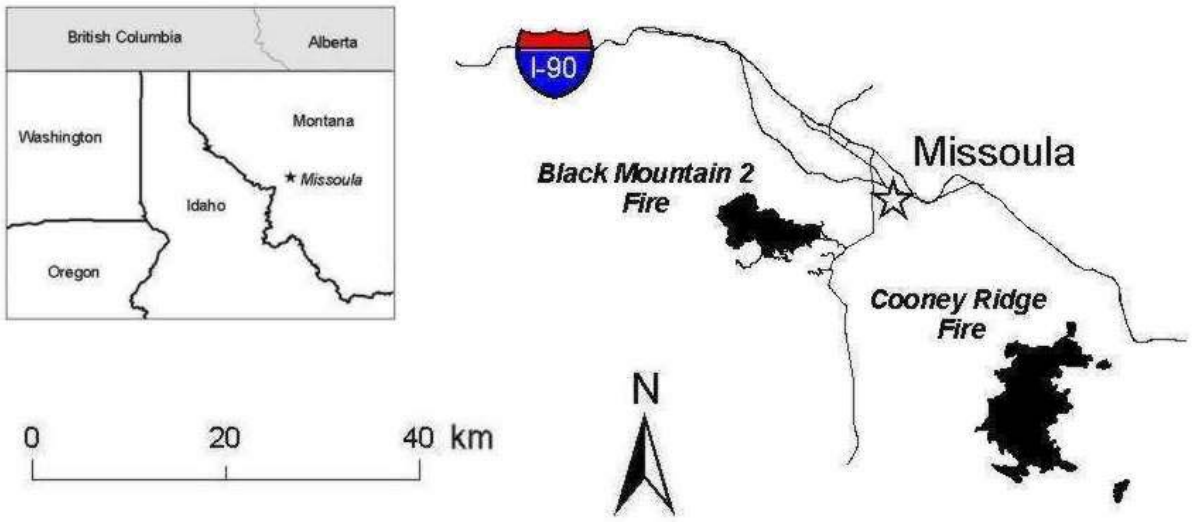

Figure 1. Location of the Black Mountain Two and Cooney Ridge wildfires in western Montana.

METHODS

Satellite Image Processing

RSAC uses the NBR or, if pre-fire imagery is also available, the dNBR, to produce BARC products. In addition to the BARC image, RSAC provides a pre-classification image called the BARC-Adjustable (BARCA). The BARCA product is simply the continuous NBR (or dNBR) values stretched across the full dynamic range (0-255). Jenks Natural Breaks logic is used to assign break points to the continuous BARCA variable and produce the categorical BARC variable. The BARCA product allows BAER teams or other users to assign their own break points based on their own ground observations.

After classifying the BARC image, RSAC overlays the National Land Cover Database (NLCD) vegetation layer. Burned grasslands, for example, are often misclassified as "high" despite the fact that grasslands rarely burn severely, and so cause little concern for BAER teams. RSAC uses the NLCD GIS overlay to catch any grassland areas classified as "high" during the NBR process and reclassifies them as "low." For the Black Mountain Two and Cooney Ridge wildfires, the NLCD vegetation overlay led to no modifications of the BARC product.

A post-fire SPOT 4 XS image (1 Sep 2003) was used to produce BARC and BARCA products from NBR values from both the Cooney Ridge and Black Mountain Two fires (Figure 2). Pre- and post-fire Landsat 5 TM images (10 Jul 2002 and 31 Aug 2003, respectively) were used to produce BARC and BARCA products from dNBR values for the Cooney Ridge fire. SPOT 4 has the advantage of being pointable, enabling simultaneous acquisition of the Black Mountain Two and Cooney Ridge fires. Unfortunately, Landsat 5 is not pointable, so the Landsat-derived BARC and BARCA products include only the Cooney Ridge fire, since the Black Mountain Two fire was situated just outside the image extent.

The Black Mountain Two and Cooney Ridge wildfires were advantageous for comparing SPOT-derived NBR values to Landsat-derived dNBR values because the SPOT and Landsat source images were acquired only a day apart. Furthermore, both of these wildfires occurred within a similar time frame and under similar fire weather conditions, and both produced a mosaic of severities to sample in the field.

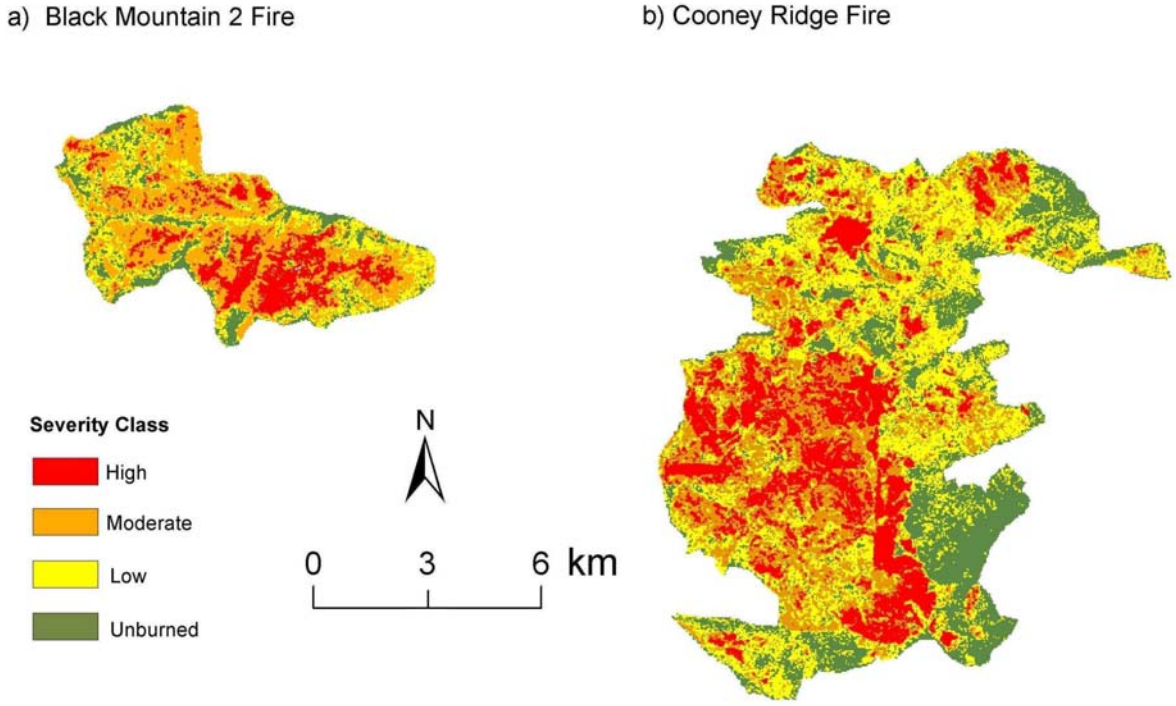

Figure 2. Burned Area Reflectance Classification (BARC) Maps of the Black Mountain Two and Cooney Ridge wildfires, from a 1 Sep 2003 SPOT-XS image.

Field Measurements and Analysis

Field data for this analysis were gathered between 11 Sep and 13 Oct 2003 at ten sites. Four sites were located at Black Mountain Two (1 in high, 1 in moderate, and 2 in low severity) while six sites were located at Cooney Ridge (1 in high, 2 in moderate, and 3 in low severity). Sites were randomly located 80-300 m from an access road, in a large patch of what was viewed as a broadly representative severity type. Burned sites with predominantly green tree crowns were classified as low, with predominantly brown crowns as medium, and with predominantly black crowns as high. More low severity sites were sampled than moderate, and more moderate than high, because of prior evidence that spatial heterogeneity in burn severity characteristics increases as burn severity decreases (Turner et al., 1999).

At each site, nine plots were situated in a 120 m x 120 m cross pattern, with the two legs bisecting each other in the form of a giant 'X'. One leg was oriented along the prevailing slope and the other leg was oriented perpendicular to it, across the slope. A plot was situated at the end of each leg, 60 m from the center plot, with another plot situated in between by 20, 30 or 40 m. Each plot consisted of 15 subplots situated in 3 rows with 5 subplots/row; rows were spaced 4 m apart while subplots in the same row were spaced 2 m apart. Distances between plots were measured using a laser rangefinder, while subplots were laid out using a cloth measuring tape. Subplots were marked with reusable pin

flags.

Ocular fractional cover estimates of rock, mineral soil, ash, litter (new and old) and any large organics were made at each 1 m^2 subplot, with the visual aid of a 1 m x 1 m quadrat constructed from pvc pipe. Percent char of each cover component was also recorded. At each plot, depth measurements of new litter (deposited post-fire), old litter and duff were made with a small ruler. Four canopy density estimates were made from the center of each plot, facing the four cardinal directions, using a convex spherical densiometer. Plot centers were geolocated by logging a minimum of 150 positions with a Trimble GeoExplorer and subsequently differentially correcting them. Subplot positions were calculated based on their known distance and bearing from plot center.

BARC data at the subplot positions were extracted from Arc/Info GRID layers using ERDAS Imagine software. Data analysis and graphing was performed using the R language with the exception of the semivariograms, which were produced with WinGsLib software. A normal score transformation, which produces a standard Gaussian cumulative distribution with mean equal to zero and variance equal to one (Deutsch and Journel, 1998), was used to normalize the data before generating semivariograms, enabling their comparison on the same graph.

RESULTS

Ten sites with 9 plots/site and 15 subplots/plot amounted to 1350 samples for comparing field and SPOT-XS BARCA data. Because the Landsat images used were limited to the Cooney Ridge fire, only the 6 Cooney Ridge sites could be compared to the Landsat-TM BARCA data (810 samples). Among the field variables, canopy density correlated most highly with the BARCA values from both sensors (Figure 3). In general, depth measurements of new litter, old litter and duff correlated more highly with the BARCA variables than the fractional cover estimates of new and old litter. Ash cover correlated with the BARCA variables most poorly. Mineral soil and rock cover correlated poorly with the BARCA variables, but when these fractions were combined into an inorganic cover fraction, the correlation to the BARCA variables improved to a level comparable to the organic cover fractions. The opposite sign of the Pearson correlation coefficients between the SPOT-XS and Landsat-TM BARCA values is simply because the former were scaled from NBR values while the latter were scaled from dNBR values.

Table 1. Pearson Correlation Coefficients Between Selected Field Variables and BARCA Values (0-255) Derived from SPOT-XS NBR and Landsat TM dNBR Values.

Field Variable	SPOT-XS NBR Correlation	Landsat-TM dNBR Correlation
Canopy Density (%)	0.8389	-0.8779
New litter depth (mm)	0.2446	-0.6260
Old litter depth (mm)	0.6282	-0.7974
Duff depth (mm)	0.5946	-0.7772
New litter cover (%)	0.4539	-0.6090
Old litter cover (%)	0.5505	-0.6474
Ash cover (%)	0.0021	0.3444
Mineral soil cover (%)	-0.3325	0.3995
Rock cover (%)	-0.5185	0.3849
Inorganic (mineral soil + rock) (%)	-0.5898	0.6091

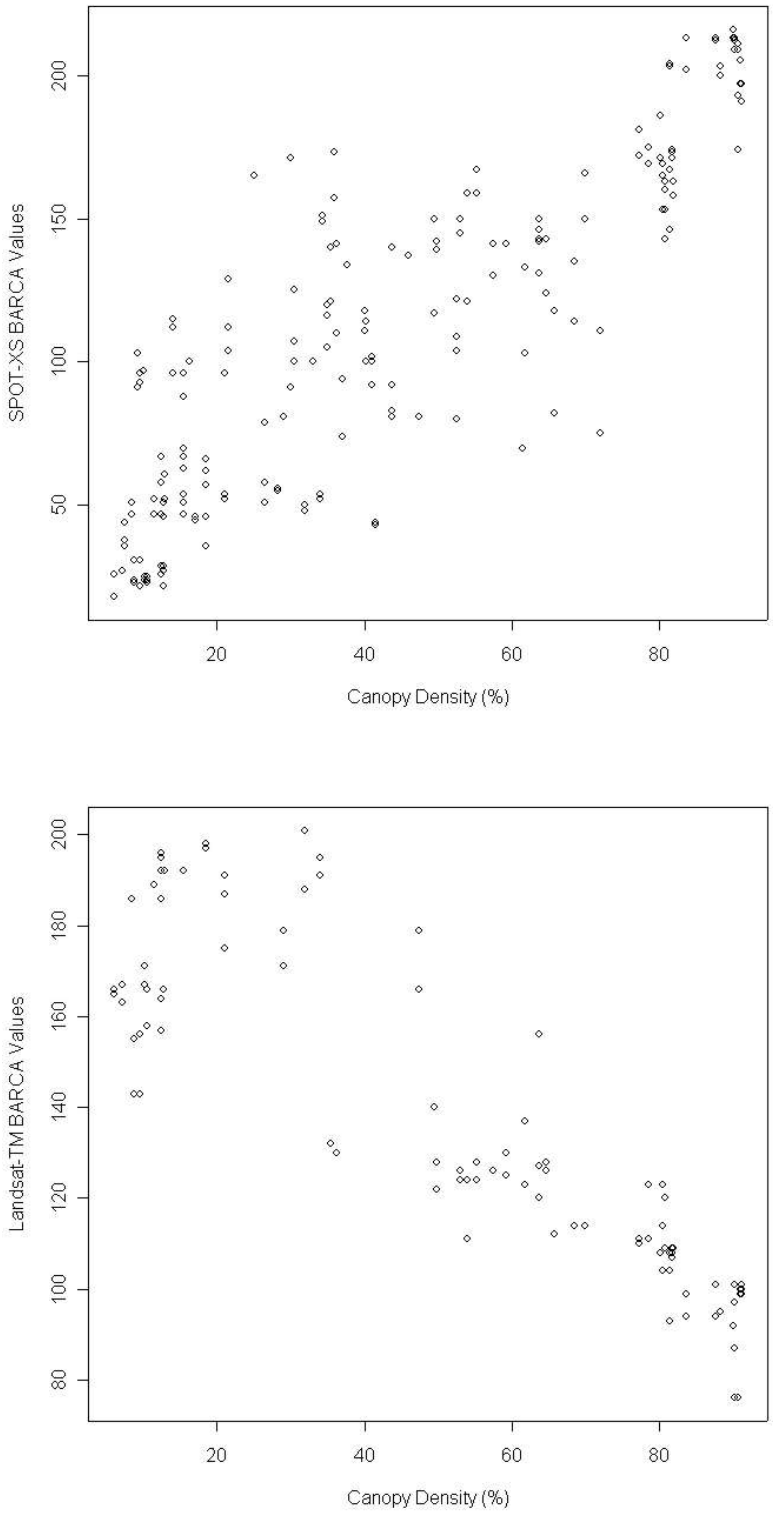

Figure 3. Scatterplots of canopy density measurements versus BARCA digital numbers derived from SPOT-XS and Landsat-TM imagery.

The range of variability in new litter, old litter and duff depth measured at low and moderate severity sites was considerably broader than at high severity sites (Figure 4). A similar pattern was observed for the old litter cover fraction, while ash cover varied much more on high severity sites, and exposed soil and rock cover varied fairly consistently across all severities (Figure 5).

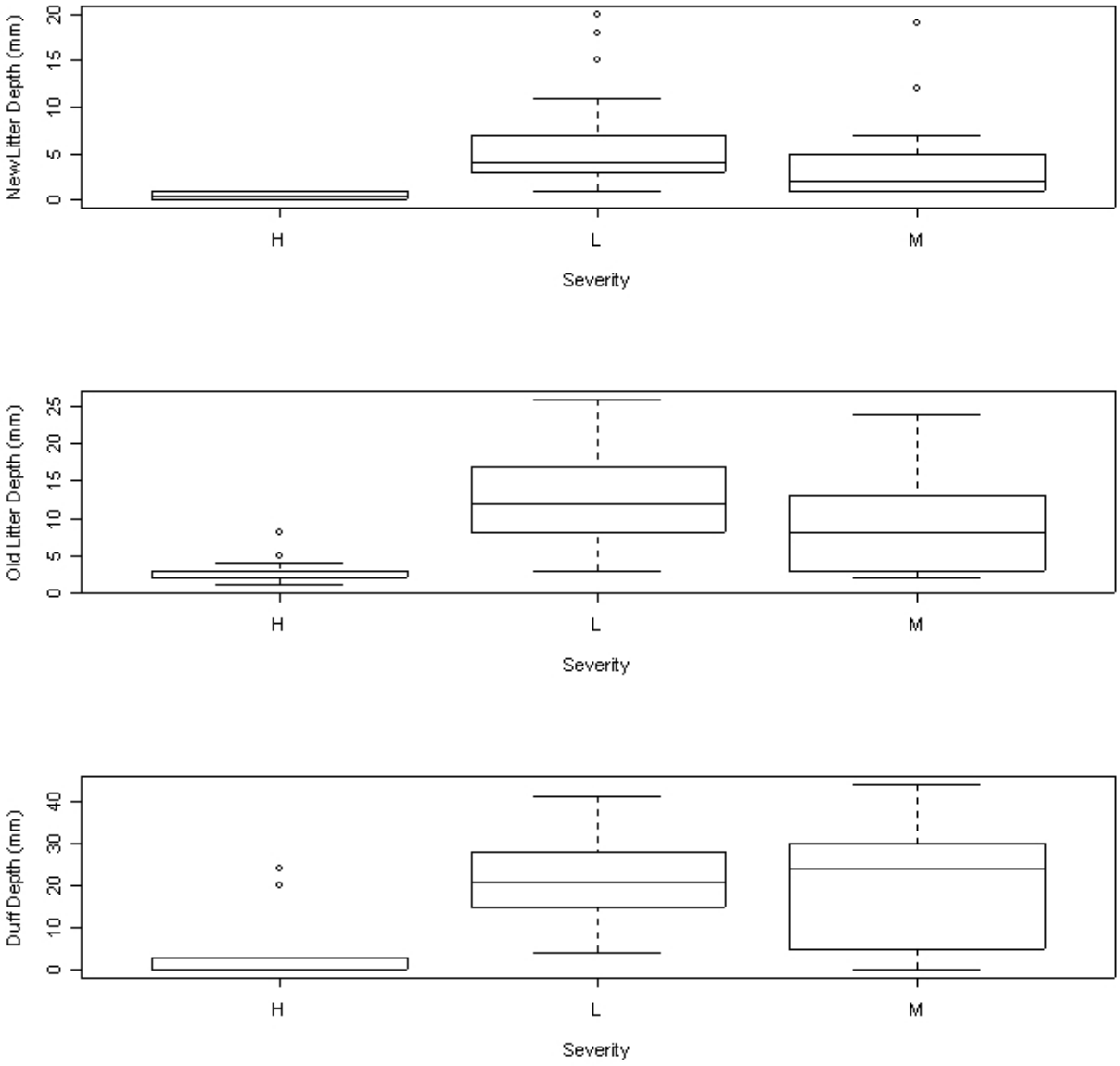

Figure 4. Boxplots of new litter, old litter and duff depths by severity class (as observed on the ground); H=High, L=Low, M=Moderate.

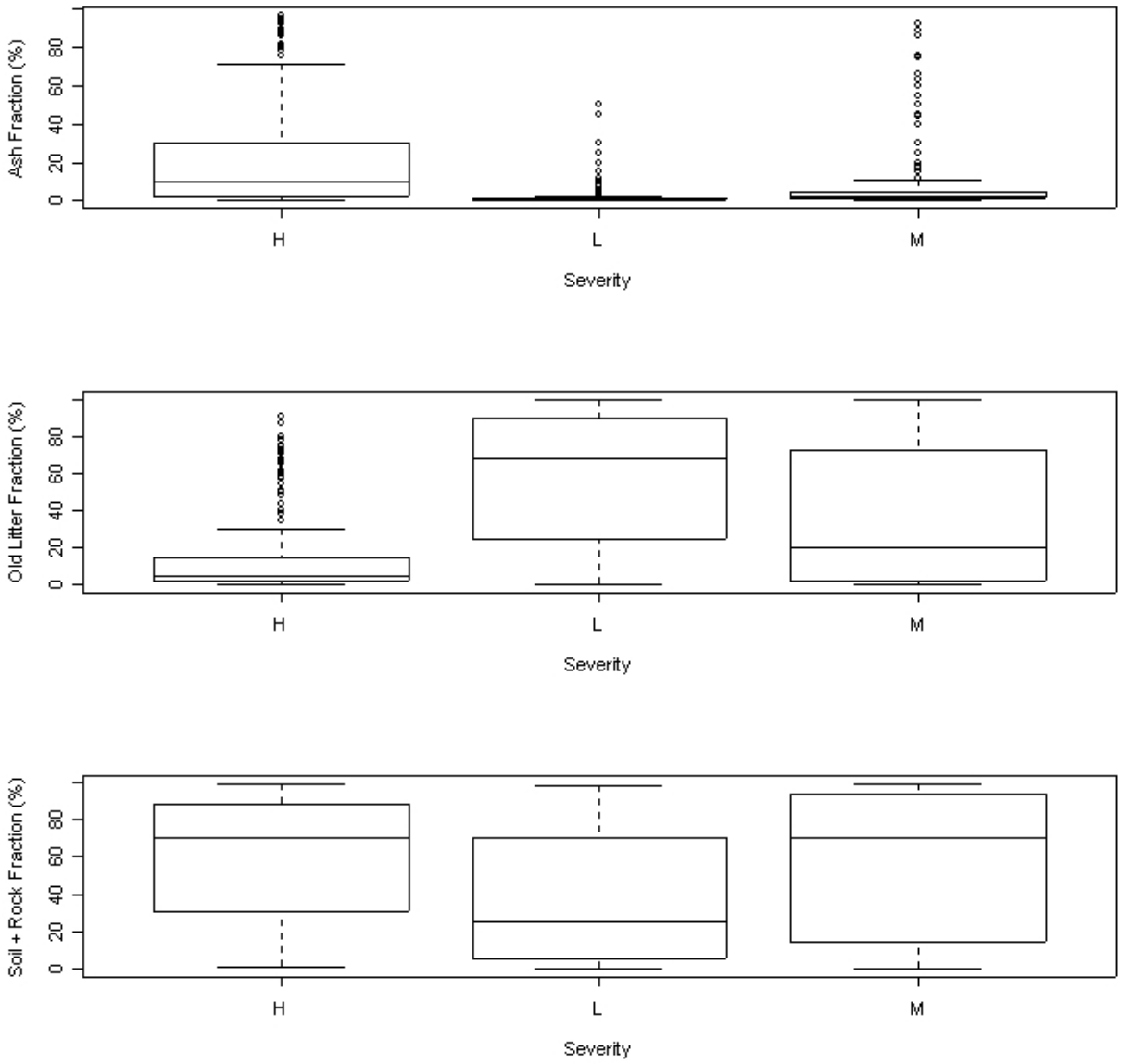

Figure 5. Boxplots of ash, organic (litter), and inorganic (mineral soil + rock) cover fractions by severity class (as observed on the ground); H=High, L=Low, M=Moderate.

At each site, the smallest lag distance separating subplots was 2 m while the largest was approximately 130 m, which defined the lower and upper distance thresholds of the semivariograms generated from the field sample data across all 10 sites (Figure 6). The fairly high nugget values of these sample semivariograms was evidence of some finer scale autocorrelation (<2 m) that was not captured at the 2 m sampling frequency. Their variable shape was evidence of spatial variation between subplots (2-12 m) and plots (12-130 m). That none of these semivariograms (with the possible exception of soil) had reached their sill was evidence of continuing spatial autocorrelation at longer lags. The reduced semivariance and smoother shape of the image-derived semivariograms was due to their much coarser resolution (20 m for SPOT-XS, 30 m for Landsat-TM).

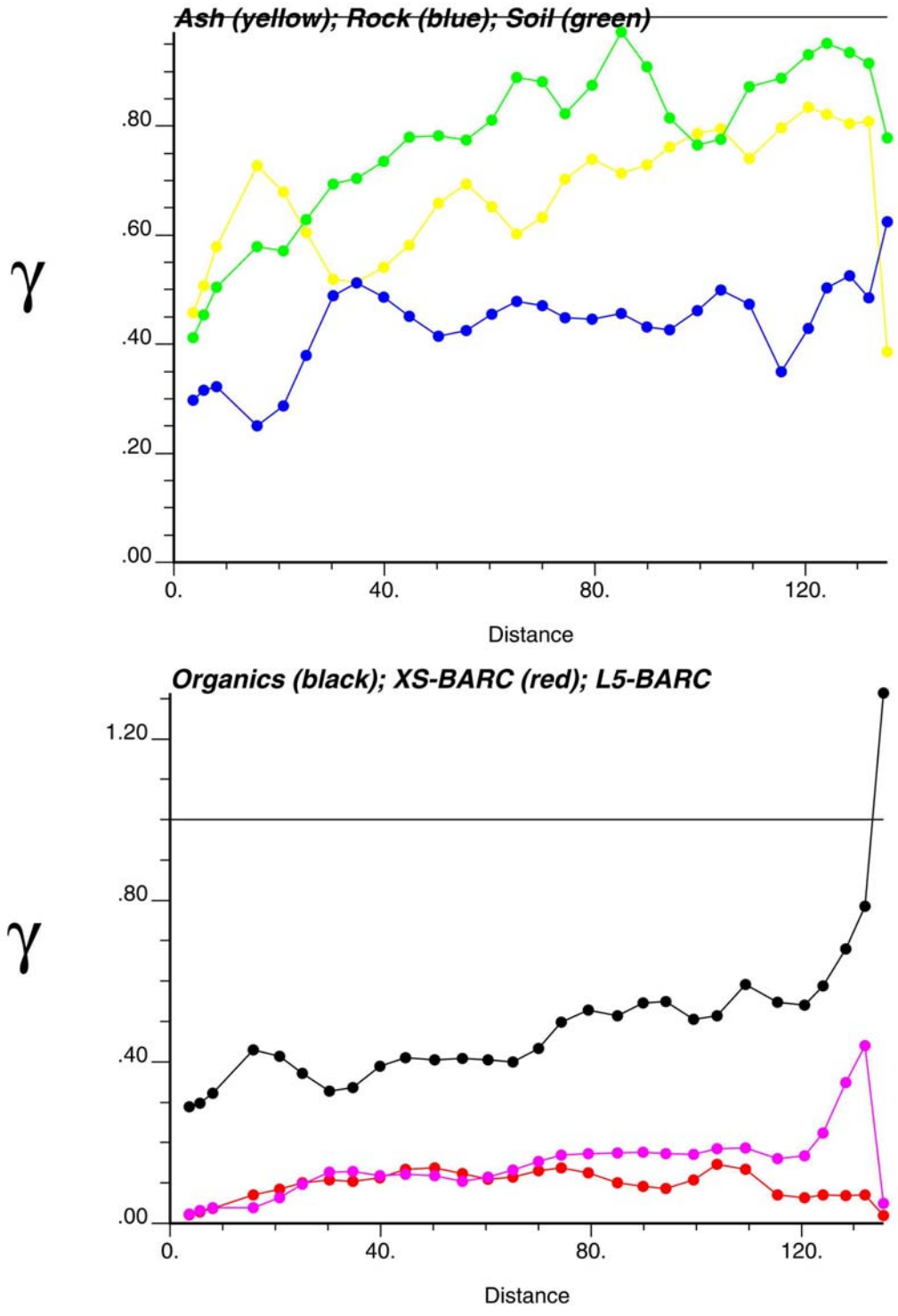

Figure 6. Semivariograms of a) ash, rock, soil and b) old litter cover fractions, and BARCA values derived from SPOT-XS and Landsat-TM imagery.

DISCUSSION

Most any type of remotely sensed imagery is more likely to capture fire effects on tree crowns than on the ground, because the canopy occludes the ground. Indeed, canopy density was a better correlate to NBR or dNBR values than any of the ground variables (Figure 3, Table 1). The better correlations between the satellite data and the new litter, old litter and duff depth data, in comparison to the new and old litter cover fractions, was surprising because the cover data were expected to have more influence on the satellite signal. Even so, the stronger relationship to the depth data is not evidence of causation (Figure 4). Mineral soil and rock behaved similarly in relation to the satellite data, which is why they were combined into a single inorganic cover fraction to present these results (Figure 5). Ash cover was perhaps the most unpredictable variable because it is redistributed by wind and water very quickly following fire. In future analyses, fire progression data will be extracted to measure time elapsed from burning until the data were acquired by the remote sensor or collected in the field. Other variables also come into play with time since burning, namely needlecast (new litter) and green vegetation regrowth. Bear grass and other vegetation had not yet resprouted at the time these satellite images were acquired and was a very minor factor when these sites were sampled in the field.

Higher semivariance in the field data was expected due to their higher sampling frequency in comparison to 20 m SPOT-XS or 30 m Landsat-TM pixels (Figure 6). Thus the satellite data was only suited for capturing spatial autocorrelation between plots. Recently acquired hyperspectral imagery of finer spatial resolution (4 m) will permit assessment of burn severity patterns at the subplot scale. Spectral mixture analysis will be applied to the hyperspectral data to remotely estimate and map cover fractions of vegetation, litter, ash, mineral soil and rock, and char (Roberts et al., 1993). Semivariograms similar to those presented here will be generated from the discontinuous cover fractions estimated in the field and the continuous cover fractions estimated by spectral mixture analysis. These semivariograms will then be fit with appropriate mathematical models to enable geostatistical simulation of burn severity patterns (Dungan, 1999). Better knowledge of burn severity patterns in relation to topographic variables should improve validation of fire behavior and spread models.

The few diagnostics presented here will be expanded to include other field variables, such as tree crown characteristics and soil water infiltration, and other remote sensing variables, such as fractional cover estimates to be derived from the hyperspectral imagery. This research will be expanded beyond the two wildfires reported here to four other wildfires sampled in 2003, as well as 2004 wildfires. Burn severity indicators will be identified that are readily mapable and scalable – that is, measurable remotely as well as on the ground. This study should lead to improved assessments of the severity of post-fire effects, including the potential for erosion and sedimentation, and thus the strategic effectiveness of post-fire rehabilitation.

REFERENCES

Bobbe, T., M. V. Finco, B. Quayle, K. Lannom, R. Sohlberg and A. Parsons (2003). Field measurements for the training and validation of burn severity maps from spaceborne, remotely sensed imagery. Final Project Report, Joint Fire Science Program-2001-2, 15 p.

Deutsch, C. V. and A. G. Journel (1998). *GSLIB Geostatistical Software Library and User's Guide.* Oxford University Press, New York, 369 p.

Dungan, J. L. (1999). Conditional simulation: an alternative to estimation for achieving mapping objectives. In: A. Stein, F. van der Meer & B. Gorte (Eds.), *Spatial statistics for remote sensing.* Kluwer Academic Publishing, Dordrecht, pp. 135-152.

Key, C. H. and N. C. Benson (2001). The Normalized Burn Ratio, a Landsat TM radiometric index of burn severity incorporating multi-temporal differencing. In preparation.

Roberts, D. A., M. O. Smith and J. B. Adams (1993). Green vegetation, non-photosynthetic vegetation and soils in AVIRIS data. *Remote Sensing of Environment* 44: 255-269.

Stone, C., A. Hudak and P. Morgan (2004). Forest harvest can increase subsequent forest fire severity. In: *International Symposium on Fire Economics, Policy and Planning: A Global Vision*, (in press).

Turner, M. G., W. H. Romme and R. H. Gardner (1999). Prefire heterogeneity, fire severity, and early postfire plant reestablishment in subalpine forests of Yellowstone National Park, Wyoming. *International Journal of Wildland Fire* 9: 21-36.